New dinuclear gold(III) complex with 1,5-naphthyridine as bridging ligand: Synthesis, characterization, DNA/BSA binding studies and anticancer activity

Snežana Radisavljević

snezana.radisavljevic@pmf.kg.ac.rs

University of Kragujevac

Dušan Ćoćić

University of Kragujevac

Biljana Petrović

University of Kragujevac

Ina Kellner

Ludwig-Maximilians-Universität München (LMU)

Ivana Ivanović-Burmazović

Ludwig-Maximilians-Universität München (LMU)

Nikola Radenković

University of Kragujevac

Danijela Nikodijević

University of Kragujevac

Milena Milutinović

University of Kragujevac

Research Article

Keywords: Gold(III), 1,5-naphthyridine, DNA, BSA, caspase

Posted Date: January 17th, 2024

DOI: https://doi.org/10.21203/rs.3.rs-3865901/v1

Additional Declarations: No competing interests reported.

Version of Record: A version of this preprint was published at Gold Bulletin on April 12th, 2024. See the published version at https://doi.org/10.1007/s13404-024-00344-8.

Abstract

With the aim to reveal the antitumor drug which possesses improved activity compared with cisplatin, we synthesized the new dinuclear gold(III) complex with 1,5-naphthyridine as bridging ligand. Further, the newly synthesized complex was characterized by various techniques to confirm the structure. The stability of this complex in water and in PBS buffer was investigated by UV-Vis spectroscopy. DNA binding studies were examined by UV-Vis, fluorescence spectroscopy and viscosity measurements. The competitive studies with EB or HOE were done by fluorescence spectroscopy. The results showed that the dinuclear gold(III) complex interacts with calf-thymus DNA (CT-DNA) *via* covalently binding mode. Furthermore, the investigated complex shows high value of binding constants for the interaction with bovine serum albumin (BSA) as well as for the interactions in the presence of site markers (eosin Y or ibuprofen). Dinuclear gold(III) complex induced remarkable cytotoxicity on HCT116 and MDA-MB-231 cancer cell lines, 24 and 72 h after treatment. The complex also showed selectivity and induced significantly lower cytotoxic activity on healthy cells compared to cancers. In support of the antitumor activity of this complex, the proapoptotic activity (via increased caspase 9 activity) and low percentages of necrosis were observed. All experimentally obtained results were corroborated by molecular docking simulations.

INTRODUCTION

It is already known that metal complexes are meaningful for biological processes, as well as in the suppression of cancer. Beside the utilization of platinum-based complex cisplatin, for more than 35 years, in the last decades ruthenium(II/III), palladium(II) and gold(III) complexes are the most investigated.[1–3]

The possibility of stabilization of gold compounds with other metals (Au-other metal) or the formation of Au-Au bond known as aurophilic interaction, are some of the many extraordinary features of gold chemistry. The most important utilization of this precious metal started in 1890, after discovering of the bacteriostatic effect of dicyanidoaurate(I) by Robert Koch. Since then, the investigation of gold(I) compounds and their usage in biological purposes increased. Nowadays, several excellent reviews summarized the pharmaceutical properties of gold(I) compounds, mechanism of their activity as well as *in vivo* investigations. Therefore, *in vivo* oxidation of gold(I) compounds leads to the formation of gold(III) compounds that can play a very important role in the biological distribution and activity of gold complexes.[4–6]

In the last two decades scientists made efforts to deeply investigate the medicinal chemistry of gold(III) complexes. It is already known that the electronic configuration of gold(III) ion ([Xe]$4f^{14}5d^{8}$, diamagnetic, low-spin configuration) showed that the gold(III) is isoelectronic with platinum(II), and due to this fact it forms four-coordinate square-planar complexes. Therefore, the similar mode of action of gold(III) and platinum(II) complexes led to the utilization of gold(III) complexes as alternatives for platinum(II) complexes. The tendency of gold(III) ions to be rapidly reduced in the presence of thiols or disulphides to gold(I) or even to metallic gold suggests that the choice of inert ligand in the coordination sphere plays

the crucial role in the developing of stable complexes.[7] In comparison with gold(I), gold(III) is a harder Lewis acid, but it is classified as a hard-soft metal ion with possibility to bind to both types of Lewis bases. Some of the most promising ligands with stabilization effect on gold(III) oxidation state are nitrogen donors (amines, pyridines, phenanthrolines, naphthyridines etc.) or sulfur donors (dithiocarbamates and thiosemicarbazones).[8]

Polynuclear metal complexes are an important part of supramolecular chemistry due to their specific coordinative bonds which connect ligands and metal centers. The nature of bridging ligands plays a crucial role in the stability of polynuclear complexes. The unique structure of pyridine led to the spread utilization in the synthesis of polynuclear complexes.[9] The most commonly used bidentate and tridentate polypyridines are 2,2'-bipyridine, 2,2';6,2"-terpyridine, 1,10-phenanthroline and their derivatives, while gold(III) complexes with these ligands are already reported.[10–12] Ligands such as pyrimidine and pyrazine are of particular interest for the synthesis of polynuclear complexes due to the coordination of metals with a greater distance between them.[13] A ligand such as 1,5-naphthyridine orients two metal centers away from one another and represents the best choice for the synthesis of dinuclear complexes. The great interest in 1,5-naphthyridines relates to good antiproliferative, antibacterial, antiparasitic, antiviral or anti-inflammatory activities. Therefore, the mentioned nitrogen-donor ligand can be used in central nervous system, for cardiovascular or hormonal diseases.[14]

Although previous work suggests the proteins are the primary target for gold(III) complexes, there is also huge importance to study the interactions with DNA molecules.[8][15, 16] DNA molecules affect cellular function and represent an excellent drug target, especially for cancer. In most previously examined cases, the drug molecules bind to DNA *via* electrostatic, hydrogen-bonding or π-π stacking interactions, while the ligands form covalent bonds. The main binding modes for small molecules, such as metal complexes, are intercalation or minor-groove binding.[17, 18] The cytotoxic effect of metal complexes usually is connected with the possibility to damage DNA, which led to the detailed investigation of interactions with this important molecule. Some published manuscripts confirmed the link between interaction of gold(III) complexes with DNA and cytotoxic effect, as well as much faster interaction with DNA in comparison with cisplatin.[19–21]

Apart from DNA, proteins are an important class of biomolecules creditable for improved biological activity of metal complexes. The osmotic pressure, blood pH, and medicine delivery to the intended targets are all regulated by serum proteins. Hence, in order to better understand the biological and pharmacological properties of any metal complex, it is crucial to investigate the interaction with serum proteins.[22] Because of its strong structural similarity with human serum albumin (HSA), bovine serum albumin (BSA), one of the most prevalent proteins in plasma, is used to study the potential mechanism of binding of metal complexes to proteins.[23]

Considering the previously mentioned research, we synthesized and characterized the new dinuclear gold(III) complex with 1,5-naphthyridine as bridging ligand. The complex was fully characterized by UV-Vis, ^{1}H NMR spectroscopy, Cryospray-MS and molar conductivity. Therefore, the stability of this complex

in water and in buffer (PBS) was investigated during the 6 hours period. Using viscosity, UV-Vis spectroscopy and fluorescence spectrometry (with EB or HOE), the interactions with the DNA molecule were examined. Furthermore, fluorescence spectroscopy was used to assess the interaction with BSA, alone or in presence of site markers, (ibuprofen or eosin Y). Computational calculations were used to validate all reported experimental data, particularly with molecular docking.

The interaction with DNA molecule was investigated using absorption spectroscopy, fluorescence spectrometry (with different kinds of DNA binders – EB or HOE) and viscosity. In addition, the interaction with BSA (without or with site markers – eosin Y and ibuprofen) was evaluated by fluorescence spectroscopy. All obtained experimental results were supported by computational calculations, specifically with molecular docking.

EXPERIMENTAL

Chemicals

Potassium tetrachloridoaurate(III) ($K[AuCl_4]$), 1,5-naphthyridine and all other chemicals were commercially available and used without purification. Ethidium bromide (EB), calf thymus DNA (CT-DNA), 2-(4-hydroxyphenyl)-5-[5-(4-methylpipera-zine-1-yl)-benzimidazo-2-yl]-benzimidazole (HOE), bovine serum albumin (BSA), eosin Y and ibuprofen were obtained from Sigma Chemicals Co. (USA).

The stock solution of CT-DNA was prepared in physiological phosphate buffer (PBS). The purity of CT-DNA solution was examined by measuring the absorbances at 260 and 280 nm and ratio A_{260}/A_{280} was calculated. The solution gave a ratio *ca.* 1.8–1.9, indicating that the DNA was sufficiently free of protein, while for calculation of the concentration of CT-DNA the molar extension coefficient 6600 M^{-1} cm^{-1} was used.[24, 25]

Stock solutions of EB/HOE, BSA and eosin Y/ibuprofen were prepared by dissolving certain amounts of solid components in PBS buffer to get concentrations of 1×10^{-3} M, 2×10^{-6} M and 5×10^{-4} M, respectively. All stock solutions were stored in the refrigerator and used within 5 days. The obtained data were collected and analyzed using the Microsoft Excel 2007 and OriginPro 8.5 programs.

The supplier of Dulbecco's Modified Eagle Medium (DMEM) was GIBCO, Invitrogen, USA. Acridine orange (AO) was acquired from Acros Organics, New Jersey, USA, and ethidium bromide (EA) from SERVA, Germany. The caspase 8 colorimetric assay kit was obtained from RD Systems, and Thermo Scientific, USA was the source of the caspase 9 primary antibody, secondary antibody coupled with Cy3, and diamidino-2-phenylindole (DAPI).

Instrumental methods

The ^1H NMR spectrum was aquired on a Bruker Avance 200 MHz spectrometer using trimethylsilylpropionic acid as reference. The Perkin-Elmer Lambda 35 double beam spectrophotometer

was used for recording the UV-Vis spectra. Quartz cuvettes with 1.0 cm path-length and volume of 3 ml were used for all UV-Vis experiments. Fluorescence spectra were obtained on a RF-1501 PC spectrofluorometer (Shimadzu, Japan) with emission and excitation bandwidths of 10 nm. In order to obtain the cryospray-ionization mass spectrum (CSI-MS), and confirm the structure of dinuclear gold(III) complex, the UHR-TOF Bruker Daltonik maXIs plus mass spectrometer with ESI-quadrupole time-of-flight (qToF) was used. The spectrometer has a resolution of at least 60000 (FWHM) and was coupled to a Bruker Daltonik Cryospray unit. The source voltage was 4.0 kV and detection was done in the positive mode. The drying gas (N_2), which facilitates solvent removal, was held at − 35°C and the nebulizer gas was held at − 40°C. The MS was calibrated prior to each experiment via direct injection of an Agilent ESI-TOF low concentration tuning mixture, which provides singly charged peaks up to *m/z* 2700 in both ion modes. The sample was dissolved in HPLC grade acetone at a concentration of 10^{-4} mol L^{-1} and directly injected at a flow rate of 240 mL h^{-1}. The measured data were processed and analysed with Bruker DataAnalysis. The freshly prepared solution in acetone (1×10^{-3} M) was used to measure the molar conductivity at 25°C on Crison EC-Meter Basic 30+. The relation $\Lambda_m = K/C$ was used to calculate the molar conductivity of complex.

Synthesis of gold(III) complex

The solution of 0.06 mmol of 1,5-naphthyridine (8.6 mg) in 3.0 ml of absolute methanol was added to the solution containing 0.13 mmol of potassium tetrachloridoaurate(III) (50 mg) dissolved in 2.0 ml of absolute methanol. The mixture prepared in this way was left stirring in the dark at the room temperature for 3 hours. This solution was filtered due to the presence of yellow precipitate and left in the dark at room temperature. After few days precipitate was collected and measured. The yield was 73.9% (71 mg).

^{1}H NMR (CD_3COCD_3): 8.24–8.28 ppm (dd, H7); 8.40–8.44 ppm (dd, H3); 9.08–9.12 ppm (d, H4); 9.28–9.32 ppm (d, H8); 9.35 ppm (dd, H6) and 9.85 ppm (dd, H2); UV-vis (H_2O, λ_{max}, nm): 265, 305, 315; UV-vis (PBS, λ_{max}, nm): 265, 300, 310; Cryospray MS (*m/z*) $[C_8H_6N_2Au_2Cl_5]^+$ 700.8246; molar conductivity ($\Omega^{-1}cm^{-1}mol^{-1}$; acetone) 36.2.

Stability of complex in aqueous and in buffer solution

UV-Vis spectrophotometer was used to analyze the stability of the complex in water and in PBS solution. A certain amount of the complex was dissolved in the smallest possible amount of acetone and filled up to 5 ml with water or PBS to get the concentration 1×10^{-4} M. Subsequently, this freshly prepared solution was used to make a diluted complex solution (5×10^{-6} M). Electronic spectra were collected over 6 hours at room temperature.

DNA-binding studies

Absorption spectroscopic studies

UV-Vis spectroscopy was used with the aim to investigate the possibility of binding of gold(III) complex toward CT-DNA. In order to calculate the binding constant (K_b) of the dinuclear gold(III) complex with CT-DNA, absorption titrations were performed with a fixed concentration of complex and different concentrations of CT-DNA stock solution. The spectra were recorded immediately after adding certain amount of CT-DNA solution, because of very fast reaction with gold(III) complex. The fixed concentration of the complex was 13.5 μM while the concentrations of CT-DNA were in the range between 6.72–65.5 μM (r up to 5). For every ratio, effect of dilution was calculated. All spectra were recorded in PBS buffer.

The value of binding constant, K_b, was calculated using Eq. (1):[26]

$$\frac{[DNA]}{(\varepsilon_A - \varepsilon_f)} = \frac{[DNA]}{(\varepsilon_b - \varepsilon_f)} + \frac{1}{K_b(\varepsilon_b - \varepsilon_f)} \quad \text{(Eq. 1)}$$

where concentration of DNA is presented as [DNA], ε_f is the extinction coefficient of the unbound complex, ε_b is the extinction coefficient of fully bound complex and $\varepsilon_A = A_{obsd}/[complex]$. The binding constant of the dinuclear gold(III) complex with DNA can be calculated by the ratio of the slope to the y intercept in plots $\frac{[DNA]}{(\varepsilon_A - \varepsilon_f)}$ *vs* [DNA].

The van't Hoff equations (Eqs. 2 and 3) were used to calculate the thermodynamic parameters in order to determine the nature of the interaction between CT-DNA and dinuclear gold(III) complex:

$\ln K_b = -(\Delta H^0/RT) + (\Delta S^0/R)$ (Eq. 2)

$\Delta G^0 = \Delta H^0 - T\Delta S^0 = -RT \ln K_b$ (Eq. 3)

where ΔH is the change of enthalpy, R is the universal gas constant, T is the temperature in K, ΔS is the change in entropy and ΔG is the Gibbs free energy.

Ethidium bromide (EB) or HOE displacement studies

Fluorescence emission spectroscopy was used in order to investigate the EB-competitive or HOE-competitive studies of newly synthesized gold(III) complex. The absorption titrations were performed with the aim to investigate the possibility of gold(III) complex to replace EB or HOE. All experiments were done in the same way, by mixing the constant concentration of EB/HOE and CT-DNA with the increasing concentrations of investigated complex. The fixed concentration of EB/HOE and CT-DNA was 6.73 μM, while the concentrations of complex were in the range between 1.33–13.9 μM (r up to 2.4) including the dilution. The excitation wavelength and emission range depend on the competitive studies, the excitation wavelength was 527 nm for EB and 346 nm for HOE, while emission range was 550–750 nm for EB and 360–600 nm for HOE. The Stern-Volmer equation (Eq. 4) was used with aim to analyze the collected results:[22]

$$\frac{Io}{I} = 1 + K_{SV}[Q]$$ (Eq. 4)

where I_0 and I are the emission intensities in the absence and in the presence of dinuclear gold(III) complex, K_{sv} is the quenching constant and [Q] is the final concentration of the quencher.

Viscosity measurements

The solutions with fixed concentration of CT-DNA and different concentrations of newly synthesized gold(III) complex were prepared with the aim to investigate the viscosity. For each sample flow time was measured five to seven times (depending on the sample) to calculate the average flow time. The collected data were presented as $(\eta/\eta_0)^{1/3}$ against *r*, where η_0 is the viscosity of DNA without complex and η is the viscosity of DNA in the presence of complex. Furthermore, the flow time of the buffer (t_0) was used to correct the flow time of the DNA-containing solution (t) using the equation $\eta = (t\text{-}t_0)/t_0$.

Albumin-binding studies

Fluorescence emission spectroscopy was used with the aim to investigate possible binding mode of dinuclear gold(III) complex to bovine serum albumin (BSA) with or without site markers, eosin Y or ibuprofen. The excitation wavelength of 295 nm and range between 300–500 nm were used to obtain the fluorescence spectra. In order to calculate BSA binding constants and parameters, titrations were done with fixed concentrations of BSA/eosin Y/ibuprofen (2 μM) while the concentrations of complex were in the range between 0.398–3.47 μM (r up to 1.8 including the dilution). The same experimental conditions were used to check the fluorescence emission of the complex in buffer solution and no emission was detected. Stern-Volmer equations (Eqs. 5 and 6) were used in order to calculate the binding parameters toward BSA:

$I_0/I = 1 + k_q\,\tau_0\,[Q] = 1 + K_{sv}\,[Q]$ (Eq. 5)

$K_{sv} = k_q\,\tau_0$ (Eq. 6)

where I_0 and I are the fluorescence intensities of BSA in the absence and in the presence of quencher, k_q and K_{sv} are the quenching rate constant and Stern-Volmer quenching constant, τ_0 is average lifetime of BSA without quencher and [Q] is the final concentration of the quencher.

Hills equation (Eq. 7) was used for static quenching interaction with the aim to obtain the number of binding sites in the biomolecule (*n*) as well as the binding constant (K):

$\log[(I_0/I)/I] = \log K + n\log[Q]$ (Eq. 7)

Molecular docking simulation

Vibration frequencies were calculated and the structure of the dinuclear gold(III) complex was optimized by utilizing a B3LYP functional[27] in conjunction with the def2-SVP basis set[28, 29] that was

implemented in the GAUSSIAN suite program.[30] DNA, BSA, and Bcl-2 molecule structural fragments were coupled with gain structures. The protein data bank (PDB) (http://www.rcsb.org) was the source of the canonical B-DNA (PDB ID: 1BNA), DNA with an intercalation gap (PDB ID: 1Z3F), BSA (PDB ID: 4F5S), and Bcl-2 (PDB ID: 2W3L). Molecular docking simulation was performed based on already published procedure and docking parameters were the same as previously published.[31]

Cell culturing

The colorectal carcinoma (HCT116) and the breast cancer (MDA-MB-231) cell lines were purchased from the ATCC (Manassas, VA, USA). HaCaT cells, human skin keratinocytes, were purchased from CLS (Eppelheim, Germany). They were cultured at standard experimental conditions and used for experiments at 70–90% of confluence.[32] Cytotoxicity was determined 24 and 72 h after treatment, while all other experiments were done at 24 h.

Cytotoxic activity - MTT assay

The cytotoxicity of dinuclear gold(III) complex on HCT116 and MDA-MB-231 carcinoma and HaCaT cells was measured using MTT assay, before reported in detail.[33] An assay measures the colour reaction – forming the blue formazan due MTT reduction via dehydrogenase in mitochondria of live cells, reflecting the cell viability/percent of cytotoxicity indirectly. The dinuclear gold(III) complex was used in concentration range of 1-200 μM, while samples in only the DMEM were a controls (non-treated cells). The IC_{50} values, concentrations that inhibit 50% cell growth, were calculated in CalcuSyn.

Cell death determination

Observation of the cell death was performed when HCT116 and MDA-MB-231 cells were stained with two fluorescent colours - acridine orange and ethidium bromide.[34] Morphology of the cells and coloured fluorescent signal were used for observation. Dinuclear gold(III) complex (IC_{50} value in μM, observed on MTT test for individual cell line) was applied to cells, while samples in only the DMEM were a controls. Double stained cells (over than 600 cells per sample) were counted, according to colour and morphological shape into viable, apoptosis in early and late stage and necrotic cells under the fluorescent microscope (Ti-Eclipse, Nikon), 400× magnification.

Determination of caspase 8 activity

For determining an activity of caspase 8 the colorimetric assay kit was used, with the protocol of the manufacturer (R&D Systems), described in our published report.[[32]] HCT116 and MDA-MB-231 cells were maintained in 25 cm^2 bottle (10^6 cells/bottle) and treated with IC_{50} concentration of dinuclear gold(III) complex, while in the control cell flask the medium was replaced.

Determination of Caspase 9 protein expression

Protein expression of caspase 9 was determined by immunocytochemistry. The step-by-step protocol has been previously published.[35] The dinuclear gold(III) complex was applied in concentration of IC_{50}

values, while samples in only the DMEM were a controls. The secondary antibody was conjugated to Cy3 and red stained, while the nuclei were blue (stained with DAPI). Relative fluorescence signal on micrographs of treated and control samples (more than 30 cells per sample were observed) was measured in ImageJ software (http://rsb.info.nih.gov/ij/).

Statistics

The data are expressed as values of three separate experiments, and present as mean ± standard error, calculated in the software (SPSS for Windows, ver. 17, 2008, Chicago, IL). The one-way ANOVA test was used for determining the statistical significance (p-value < 0.05).

RESULTS AND DISCUSSION

In this work, we prepared a new dinuclear gold(III) complex $[Au_2(1,5\text{-naph})Cl_6]$, where 1,5-naph is 1,5-naphthyridine, according to the procedure presented in Scheme 1.

The structure of the complex was characterized by different spectroscopic techniques such as: UV-Vis, ^{1}H NMR spectroscopy, Cryospray-MS and molar conductivity. All recorded spectra are presented in ESI, Figures S1-S3.

In the ^{1}H NMR spectrum of dinuclear complex $[Au_2(1,5\text{-naph})Cl_6]$ six signals in aromatic region correspond to the symetrical 1,5-naph ligand (ESI, Fig. S1), while the signals of H7 atoms appeared at 8.24–8.28 ppm, of H3 at 8.40–8.44 ppm, of H4 at 9.08–9.12 ppm, of H8 at 9.28–9.32 ppm, of H6 at 9.35 ppm and the signal of one H2 at 9.85 ppm.

The UV-Vis spectra of dinuclear gold(III) complex was recorded in water and in PBS buffer (ESI, Fig. S2). The values of λ_{max} are almost identical (265, 305 and 315 nm in water; 265, 300 and 310 nm in PBS). The band at 265 nm corresponds to the intra-ligand ($\pi \rightarrow \pi^*$) charge transfer, while the bands at 300/305 nm and 310/315 nm are described as ligand-to-metal charge transfer (LMCT).[23]

While the dinuclear gold(III) complex is neutral, the dissociation of one chloride ligand results in the corresponding molecular ion $[C_8H_6Au_2Cl_5N_2]^+$ (*m/z* 700.8246), which could be detected by Cryospray-MS analysis. Its recorded isotope pattern also fits the simulation, supporting this assignation (ESI, Fig. S3)

The calculated molar conductivity value confirmed the non-electrolyte nature of the complex.[36]

Stability of complex in aqueous and in buffer solution

The stability of dinuclear gold(III) complex in water and in PBS was analyzed by UV-Vis spectrophotometry. According to the UV-Vis spectra (ESI, Fig. S4, left), the modification in the shape of spectra was not observed, while a significant decrease in the intensity of the characteristic bands was presented. It can be concluded that in the water solution the investigated gold(III) complex undergoes potential hydrolysis of gold(III)-halide bonds.[10] After six hours in PBS buffer, the other UV-Vis spectrum

revealed very small change in the absorption maxima (ESI, Fig. S4, right), indicating its very good stability, which is crucial for other investigations and possible further usage of this dinuclear complex.

DNA binding studies

It is already known that DNA represents the primary biological target for many transition metal ion complexes, as well as there are two possible binding modes described as covalent and non-covalent interactions. The first binding mode, covalent binding, involves the formation of bond between DNA (exactly N7 atom of guanine) and complex compound. The second binding mode, non-covalent interactions, includes intercalative, electrostatic and surface (groove) bindings.[22] The most common methods used to determine the possible binding mode of metal complexes toward DNA are UV-Vis spectroscopy and fluorescence spectroscopy. In order to investigate the binding mode of dinuclear gold(III) complex and CT-DNA, in the scope of this work, UV-Vis, fluorescence quenching and viscosity measurements were done.

The absorption titration of dinuclear gold(III) complex in PBS buffer was done by using a fixed concentration of complex (13.5 μM) to which an increasing concentration of CT-DNA was added directly in the cuvette (6.72–65.5 μM; r up to 5). The spectra were obtained at three different temperatures. Addition of CT-DNA to the solution of dinuclear gold(III) complex led to an increase in the absorption intensities (hyperchromism) at 258 nm (Fig. 1). The obtained results can suggest the presence of synergic non-covalent interactions.[26]

The intrinsic binding constant (K_b) was calculated by using Eq. 1 (see experimental), while the thermodynamic parameters were calculated by using equations 2–3 (see experimental) and all calculated values are summarized in Table 1.

The high values of intrinsic binding constant, K_b, at all three temperatures indicate the very strong binding of dinuclear gold(III) complex to CT-DNA. Recio Despaigne et al. reported that the intrinsic binding constant for classical intercalation EB is $(1.23 \pm 0.07) \times 10^5\ M^{-1}$.[37] According to the obtained results it can be concluded that dinuclear gold(III) complex exhibits a higher value of binding constant, while the differences between K_b suggest that complex has an impact on DNA which is dependent on the temperature.

Table 1
DNA-binding constant (K_b) and thermodynamic parameters for CT-DNA/complex system

T	$K_b \times 10^5$	R^2	ΔG^0	ΔH^0	ΔS^0	R^2
(K)	(M^{-1})		($kJmol^{-1}$)	($kJmol^{-1}$)	($JK^{-1}mol^{-1}$)	
298	1.51 ± 0.04	0.9911	-104.69 ± 0.02	-37.61 ± 0.05	225.1 ± 0.2	0.9852
303	1.82 ± 0.04	0.9910	-105.82 ± 0.04			
310	2.71 ± 0.02	0.9964	-107.39 ± 0.03			

The values of the activation parameters (ΔH^0 and ΔS^0) can suggest the mode of binding. It is already proven that: if the values of both parameters are higher than zero the hydrophobic interactions are dominant; if the enthalpy is almost zero and entropy is higher than zero the electrostatic forces are dominant and if the values of both parameters are smaller than zero the hydrogen bonding and van der Walls forces are dominant.[38] The negative values of standard Gibbs free energy indicate that the binding between dinuclear gold(III) complex and CT-DNA occurs spontaneously.

Competitive fluorescence measurements

Competitive fluorescence measurements were performed in the presence of 3,8-diamino-5-ethyl-6-phenyl-phenantridinium bromide (ethidium bromide, EB) or a synthetic derivative of N-methyl piperazine (HOE) in order to further investigate the binding mechanism of dinuclear gold(III) complex toward CT-DNA.

EB is a classical intercalator and when intercalates into DNA base pairs it produces the significant fluorescence emission intensity. Furthermore, the decrease in fluorescence intensity is caused by the displacement of EB from EB-DNA system.[23] The fluorescence titration of EB-DNA with the increasing concentration of dinuclear gold(III) complex (1.35–13.9 μM) is shown in Fig. 2. Based on the acquired data, the decrease in fluorescence intensity at 608 nm indicates that the dinuclear gold(III) complex has the ability to remove EB from the EB-DNA system and interact with DNA, most likely by intercalative mode.[39]

In good agreement with Stern-Volmer equation (see experimental, Eq. 4), the Stern-Volmer plot I_0/I *vs.* [Q] demonstrated linear dependence. This equation was used to get the Stern-Volmer quenching constant (K_{sv}). The value is presented in Table 2. The high value for the calculated constant (10^4 M^{-1}) indicates the possibility of dinuclear gold(III) complex to replace EB and strongly bind to DNA.

Table 2
Stern-Volmer constant (K_{sv}) obtained from EB-DNA and HOE-DNA

	K_{sv} (M^{-1})	R^2
EB	$(3.94 \pm 0.06) \times 10^4$	0.996
HOE	$(7.41 \pm 0.02) \times 10^5$	0.992

HOE, synthetic derivative of N-methylpiperazine, attaches to DNA in the minor groove in a variety of ways. The high planarity of HOE led to the increase of fluorescence intensity when the increasing concentration of DNA is added. Moreover, when some transition metal ion complexes are able to bind to DNA and replace HOE, the fluorescence intensity of the HOE-DNA system decreases.[22] The fluorescence titration with the constant concentration of HOE/DNA to which increasing concentration of complex (1.35–13.9 μM) was added, showed the appreciable reduction in the fluorescence intensity at 512 nm and the increasing of the fluorescence intensity at 409 nm (Fig. 2).

The competition reaction between gold(III) complex and HOE, which resulted in the release of HOE is indicated by the addition of dinuclear gold(III) complex to HOE-DNA system. This result is evidence that the complex interacts with DNA by groove binding rather than by intercalation.[22] The obtained value of the binding constant (K_{sv}, Table 2) is 10 times higher than the constant obtained for EB, indicating that the groove binding is probably the main mode of binding.

Beside all, the observed values of constants for EB (10^4 M^{-1}) and HOE (10^5 M^{-1}) still cannot clarify the mode of binding to DNA. With the aim to further examine the possibility of binding toward DNA molecule, viscosity measurements were done. The elongation of DNA and increase of the viscosity of solution can be observed when the classical intercalator push affected base pairs of DNA away.[22] In our experiment, the viscosity of solution slightly increases (ESI, Fig. S5) with the increasing concentration of dinuclear gold(III) complex, suggesting the groove-binding mode.[40] These results are in the good agreement with previously calculated Stern-Volmer constants for HOE and EB.

Albumin binding studies

Serum albumin (SA) represents the most abundant protein in blood plasma. Bearing this in mind, the examination of interactions between different metal-based drugs and serum albumin has great importance. Furthermore, the biological activity of some original drugs can be enhanced or lost as a result of binding to this protein.

Because of their structural similarity to human serum albumin (HSA), bovine serum albumin (BSA) is the albumin that has been investigated the most.[41] Specifically, after adding a metal-based compound, BSA's fluorescence spectra may quench due to modifications in protein structure, subunit interaction, substrate binding, or denaturation.[10]

It is already known that the presence of trypthophan residues in the BSA molecule led to the appearance of intense fluorescent emission near 360 nm. However, after the addition of dinuclear gold(III) complex to the BSA solution, the decrease in fluorescence intensity was noted (Fig. 3), indicating the changes in the environment of trypthophan in serum albumin and binding of the dinuclear complex to the protein. Additionally, the band maximum was shifted from 366 nm to 363 nm (blue shift) confirming the presence of strong interactions of dinuclear gold(III) complex with the tryptophan residue of the protein.

Stern-Volmer equations (see experimental, Eqs. 5–6) were used with the aim to obtain Stern-Volmer quenching constant (K_{sv}) and quenching constant (k_q), while Hill's equation (see experimental, Eq. 7) was used to obtain the BSA-binding constant (K) as well as the number of binding sites per albumin (*n*). All calculated values are presented in Table 3, while obtained spectra and graphs are presented on the Fig. 3.

Table 3
Binding parameters for dinuclear gold(III) complex with BSA (without and with site markers)

	BSA	BSA-eosin Y	BSA-ibuprofen
$K_{sv} \times 10^5$ (M^{-1})	5.30 ± 0.07	4.11 ± 0.07	4.29 ± 0.07
$k_q \times 10^{13}$ (M^{-1} s^{-1})	5.30 ± 0.03	4.11 ± 0.03	4.29 ± 0.03
$K \times 10^6$ (M^{-1})	11.00 ± 0.07	6.46 ± 0.04	7.95 ± 0.05
n	1.27	0.4	1.21

According to the calculated quenching constant (k_q) which is higher than diverse kinds of quenching for biopolymer fluorescence (10^{10} M^{-1} s^{-1}), can be noticed the presence of a static quenching mechanism. [10] The number of binding site, *n*, suggests the single binding site in serum albumin.

Furthermore, competitive experiments with site markers were performed in order to determine the position of binding of dinuclear gold(III) complex to BSA. Site marker for site I (subdomain IIA) is known as eosin Y, while the marker for site II (subdomain IIIA) is known as ibuprofen.[38] According to the spectra presented in the Fig. 4., during the fluorescence titration the fluorescence intensity decreases, suggesting the binding of marker to BSA (see fluorescence intensity of BSA without and with markers) and after that competition reaction between gold(III) complex and corresponding marker. In Table 3 it can be seen that the binding constants have similar value in the presence of eosin Y and ibuprofen, while the constant in the presence of ibuprofen is slightly higher. This result can be explained by the existence of competitive reaction between dinuclear gold(III) complex and ibuprofen in binding to BSA molecule, confirming the binding of complex to site II of BSA.

Gold(III) complex cytotoxicity

The tested dinuclear gold(III) complex significantly decreased the viability of HCT116 and MDA-MB-231 cells in most administered doses, as shown by cell viability curves (ESI, Figure S6). The observed IC_{50}

values were used as a parameter for cytotoxicity (Table 4). They show that the dinuclear gold(III) complex induces significant cytotoxicity on investigated cell lines compared to commercially used cytostatic (data observed from Genomics of Drug Sensitivity in Cancer, https://www.cancerrxgene.org/). The time-dependent cytotoxicity was observed on HCT116 cells, while dinuclear gold(III) complex induces stronger activity after 24 h on MDA-MB-231 cells. The IC_{50} values on normal human keratinocytes show that the dinuclear gold(III) complex showed selectivity and induces lower cytotoxic activity on healthy cells compared to cancer.

Table 4
The cytotoxicity of dinuclear gold(III) complex - IC_{50} values (μM) on selected cell lines

	Dinuclear gold(III) complex (μM)	
Cell line	**24 h**	**72 h**
HCT116	12.59 ± 1.96	1.76 ± 0.03
MDA-MB-231	43.95 ± 1.63	76.31 ± 0.65
HaCaT	136.12 ± 2.34	174.87 ± 0.85

Gold(III) complex induces apoptosis

The results of AO/EB double staining showed that dinuclear gold(III) complex decreased percentage of viable cells in both investigated cell lines compared to untreated control and activate apoptosis dominantly, compared to other cell deaths (Table S1, ESI and Fig. 5). Among different detectable stages and types of cell death (apoptosis *vs* necrosis), the highest percentages of early apoptotic cells were detected, followed by late apoptosis compared to spontaneous in control cells. Red coloured necrotic cells were observed in a low percentage. On presented micrographs (Fig. 6) the specific apoptotic morphological changes were clearly visible in treated HCT116 and MDA-MB-231 cells. Those are membrane blebbing, cell condensation, volume reduction, more intensive green fluorescence which indicates apoptosis in early stage or more visible changes in condensation of nuclei, coloured orange which indicates apoptosis in late stage.

Molecular mechanism of induced cell death – apoptosis

To underline the mechanism of apoptosis induction in tested cancer cells, we examined the level of caspase 8 activity, the initial caspase in the external apoptotic pathway. Caspase 8 activity was not significantly altered in both cell lines treated with gold(III) complex, compared to control (Fig. 7).

The caspase 9 protein expression, as the initial caspase in the mitochondria-dependent apoptotic pathway was determined. The level of caspase 9 on micrographs and result of relative cell fluorescence shows significant change in caspase 9 expressions in both treated cells, compared to control (ESI, Fig. S7 and Fig. 8).

In a large number of ongoing studies novels biologically active compounds designed as antitumor agents have been reported, including metal-based cancer drug candidates. Many of them indicate gold-based drugs anticancer activity and their potential importance in cancer therapy, which primarily means reducing the harmful effects that occur with available cytostatics.[42–45] As an antitumor agent, metal-based complexes, according to the latest research, behaved much better in terms of the appearance of resistance, in comparison with platinum-based complexes, such as cisplatin, oxaliplatin, etc.[46] Concretely, gold complexes are most often combined with biologically active ligands, precisely to prevent the side effects, like isoquinoline,[46] thiohydantoin[10][47], and many others. The anticancer activity of different gold complexes is detected on many cancer cell lines.[48] Our previous results also shows cytotoxicity of tetra- and penta-coordinated gold(III) complexes[10] and apoptotic activity of complexes with phenanthroline on colon and breast cancer cells.[47] Results of this research shows that dinuclear gold(III) complex processes a remarkable cytotoxicity on colon (HCT116) and breast cancer cells (MDA-MB-231), which was indicated by observed IC_{50} values. In addition to cytotoxicity, the selectivity in action was observed and noticeably higher values on HaCaT healthy cells. In our previous results the selectivity of gold(III) complexes with thiohydantoin ligands was not observed, considering the cytotoxicity on healthy cells.[10] However, the other authors reported that their new-synthetized gold complex is toxic only in high doses (100μM).[49]

These results indicate that novel dinuclear gold(III) complex processes cytotoxic activity by inducing the apoptosis in both investigated cell lines (in concentration of IC_{50} value). According to literature data, many other gold complexes also caused a proapoptotic effect on different cancer cell lines.[50] When we examined the mechanism of induced apoptosis in more detail, it was shown that novel dinuclear gold(III) complex induce apoptosis in HCT116 and MDA-MB-231 cells through the internal apoptotic pathway (due to increased caspase 9 expression), without the activation of the external, receptor-mediated pathway. Literature data about proapoptotic mechanism of some gold derivates, also implies activation of caspase-dependent apoptosis,[51] and activation of internal pathway through affecting of mitochondrial membrane potential.[50] This result implies that molecules involved in the internal apoptotic pathway may be an important therapeutic target.

Molecular docking analysis

At the atomic level, structural compatibility between tiny and large molecules can be accurately predicted by molecular docking simulations. MVD-related scoring functions, from which MolDock and Hbond are regarded as the most relevant, obtained after docking simulation can be a marker of the affinity of the parent scaffolds and their integration complexes with a target macromolecule, in case of our study with DNA, BSA and Bcl-2. The optimal feasible geometry for the investigated complex inside the DNA double helix, for binding inside BSA cavities (in subdomains IIA and IIIA), and for binding with Bcl-2 protein was suggested by using the top-ranked poses for the investigated complex with the lowest docking values.

The complex under study was docked into a rigid structure of DNA fragments, displaying either (i) DNA with an intercalation gap (PDB 1Z3F) or (ii) canonical B-DNA (PDB 1BNA). As a result, two different kinds

of interactions (minor groove and intercalation) were investigated and assessed. The crystal structure of a synthetic DNA dodecamer is fragment 1BNA. Simultaneously, 6 base pairs of DNA fragments in combination with the intercalating anticancer agent ellipticine (which was removed before docking) have been presented as 1Z3F. Table 5 displays the top-ranked poses based on the scoring functions that were applied, and Fig. 9 displays the best-docked poses.

Table 5
MVD-related scoring function values for DNA docking with investigated dinuclear gold(III) complex

PDB	MolDock	Rerank	Hbond	Docking
1BNA	-129.88	-84.51	0	-127.06
1Z3F	-115.59	-70.66	-0.86	-115.09

Based on MVD-related scoring functions (most notably MolDock values) presented in Table 6, the investigated complex can exhibit great structural completability with the DNA molecule structure. Considering the great planarity of the investigated dinuclear gold(III) molecular docking predicted slightly better interaction throughout minor groove binding then by intercalation, results which are in alignment with the competitive fluorescence measurements on DNA binding mode. In both interaction modes, docking simulations could not identify significant hydrogen bond formations between the dinuclear gold(III) complex and the DNA backbone.

Using molecular docking modeling, an interaction mechanism between the dinuclear gold(III) complex and BSA was also investigated. The BSA molecule's subdomains IIA and IIIB were docked too. The hydrophobic cavity located in subdomain IIA, which accommodates the drug molecule, plays a crucial role in the metabolism and movement of biomolecules. Table 6 displays the interaction results reported as top-scored values for the investigated complexes with BSA protein that were docked into binding sites IIA and IIIA, based on the scoring functions that were applied. The optimal positions based on the Hbond scoring function are displayed in ESI, Figure S8 and Fig. 10, with BSA docked into subdomains IIA and IIIA for the examined complexes.

Table 6
MVD-related scoring function values for dinuclear gold(III) complex docked into the BSA protein binding site IIA and IIIA, and binding site of Bcl-2 protein

Protein	MolDock	Rerank	Hbond	Docking	Amino acid residues [b,c]
BSA-IIA[a,b]	-73.16	-50.59	-1.14	-81.31	Trp-213, Ala-291, Arg-222(H), Ser-287
BSA-IIIA[a,b]	-82.89	-57.78	0	-90.34	Phe-403, Val-433, Asn-391, Leu-387, Arg-485, Arg-410, Ser-489, Tyr-411
Bcl-2[a,b]	-62.98	-38.42	0	-41.46	Glu-95, Leu-96
[a] According to MolDock scoring function, the best complex pose.					
[b] Best complex pose according to Hbond scoring function.					
[c] (H) indicates that the amino acid is bound to a complex by a hydrogen bond.					

The investigated dinuclear gold(III) complex is well accommodated into the binding pocket located at subdomain IIA as well as in subdomain IIIA of the BSA molecule, as can be seen from the obtained molecular docking scoring function values displayed in Table 7. Based on gain simulation results, subdomain IIIA is more favorable to host the investigated complex, results which follow the experimental competitional measurements with BSA protein. No significant possibility for forming a hydrogen bond between complex and BSA molecule was observed.

Cancer cells were shown to become more susceptible to apoptosis when small compounds were able to block the antiapoptotic Bcl-2 protein.[27] The inhibition of Bcl-2's antiapoptotic activity was the mechanism of action of these inhibitors, which relied on their binding to the binding groove in Bcl-2. Increased activity of caspase 9 and activation of inner apoptotic pathway, which was observed in induced apoptosis in both cell lines, indicates dysregulations of Bcl-2 members of protein family by investigated dinuclear gold(III) complex. A comparative molecular docking study was conducted to examine the studied complexes' capacity to bind to and inhibit Bcl-2. The purpose of this work was to evaluate for the dinuclear gold(III) complex possible structural binding affinities, mechanisms, and interactions with Bcl-2. Table 7 displays the top-ranked poses based on the scoring functions that were utilized, and Fig. 11 displays the best-docked poses of complexes with Bcl-2.

Based on the results in Table 6 all investigated dinuclear gold(III) complex can exhibit structural compatibility with antiapoptotic Bcl-2 protein. As in case of BSA protein, due to the occupancy of complex’s nitrogen atoms no possibility for forming a hydrogen bond between complex and Bcl-2 protein was observed.

Conclusion

In this study, we described the synthesis of new dinuclear gold(III) complex with 1,5-naphthyridine as bridging ligand, as well as its complete characterization (including UV-Vis, 1H NMR spectroscopy, Cryospray-MS and molar conductivity). The complex showed poor stability in water but good stability in buffer solution, which was the most important property for further investigations. According to the experimental results, obtained by using different techniques (UV-Vis or fluorescence spectroscopy and viscosity), the complex binds to DNA by groove binding, while the molecular docking simulations confirmed slightly better interaction through minor groove binding than by intercalation. Furthermore, the complex has great affinity to bind to BSA, exactly to the side II (subdomain IIIA), which was proved with molecular docking simulations. The complex exhibits high anticancer potential, due cytotoxic and proapoptotic activity on colon and breast cancer cell lines. The selectivity on cancer cells was also observed, considering the significantly higher IC50 values on normal cells.

Declarations

Author Contribution

S.R. Investigation; methodology; validation; wrote the main manuscript text; prepared all figures. D.Ć. Investigation, software. B.P. Data curation; investigation; supervision; validation. I.K. Investigation; supervision. I.I.B. Investigation; supervision. N.R. Investigation; methodology. D.N. Investigation; methodology. M.M. Investigation; methodology. All authors reviewed the manuscript

Acknowledgement

The authors are grateful to the Ministry of Education, Science and Technological Development of the Republic of Serbia (Agreement No. 451-03-68/2023-14/200122 and 451-03-47/2023-01/200122).

References

1. Cutillas N, Yellol GS, De Haro C, et al (2013) Anticancer cyclometalated complexes of platinum group metals and gold. Coord Chem Rev 257:2784–2797. https://doi.org/10.1016/j.ccr.2013.03.024
2. Frik M, Jiménez J, Vasilevski V, et al (2014) Luminescent iminophosphorane gold, palladium and platinum complexes as potential anticancer agents. Inorg Chem Front 1:231–241. https://doi.org/10.1039/C4QI00003J
3. Savić A, Marzo T, Scaletti F, et al (2019) New platinum(II) and palladium(II) complexes with substituted terpyridine ligands: synthesis and characterization, cytotoxicity and reactivity towards biomolecules. BioMetals 32:33–47. https://doi.org/10.1007/s10534-018-0155-x
4. Shaw CF (1999) Gold-Based Therapeutic Agents. Chem Rev 99:2589–2600. https://doi.org/10.1021/cr980431o

5. Berners-Price SJ (2011) Gold-Based Therapeutic Agents: A New Perspective. Bioinorg Med Chem 197–222. https://doi.org/10.1002/9783527633104.ch7
6. Fricker SP (1996) Medical uses of gold compounds: Past, present and future. Gold Bull 29:53–60. https://doi.org/10.1007/bf03215464
7. Bertrand B, Williams MRM, Bochmann M (2018) Gold(III) Complexes for Antitumor Applications: An Overview. Chem - A Eur J 24:11840–11851. https://doi.org/10.1002/chem.201800981
8. Maia PI da S, Deflon VM, Abram U (2014) No Title. Future Med Chem 13:1515–1536. https://doi.org/10.4155/FMC.14.87
9. Singh AN, Thummel RP (2009) 1,5-Naphthyridine as a new linker for the construction of bridging ligands and their corresponding ru(II) complexes. Inorg Chem 48:6459–6470. https://doi.org/10.1021/ic900400t
10. Radisavljević S, Đeković Kesić A, Ćoćić D, et al (2020) Studies of the stability, nucleophilic substitution reactions, DNA/BSA interactions, cytotoxic activity, DFT and molecular docking of some tetra- And penta-coordinated gold(iii) complexes. New J Chem 44:11172–11187. https://doi.org/10.1039/d0nj02037k
11. Casini A, Diawara MC, Scopelliti R, et al (2010) Synthesis, characterisation and biological properties of gold(iii) compounds with modified bipyridine and bipyridylamine ligands. J Chem Soc Dalt Trans 39:2239–2245. https://doi.org/10.1039/b921019a
12. Gimeno MC, López-De-Luzuriaga JM, Manso E, et al (2015) Synthesis, Photochemical, and Redox Properties of Gold(I) and Gold(III) Pincer Complexes Incorporating a 2,2':6',2"-Terpyridine Ligand Framework. Inorg Chem 54:10667–10677. https://doi.org/10.1021/acs.inorgchem.5b01477
13. Marcaccio M, Paolucci F, Paradisi C, et al (2002) Electrochemistry and spectroelectrochemistry of ruthenium(II)-bipyridine building blocks. Different behaviour of the 2,3- and 2,5-bis(2-pyridyl)pyrazine bridging ligands. J Electroanal Chem 532:99–112. https://doi.org/10.1016/S0022-0728(02)00905-1
14. Fuertes M, Masdeu C, Martin-Encinas E, et al (2020) Synthetic strategies, reactivity and applications of 1,5-naphthyridines. Molecules 25:. https://doi.org/10.3390/molecules25143252
15. Posssato B, Dalmolin LF, Pereira LM, et al (2021) Gold(III) complexes with thiosemicarbazonate ligands as potential anticancer agents: Cytotoxicity and interactions with biomolecular targets. Eur J Pharm Sci 162:. https://doi.org/10.1016/j.ejps.2021.105834
16. Casini A, Messori L (2011) Molecular Mechanisms and Proposed Targets for Selected Anticancer Gold Compounds. Curr Top Med Chem 11:2647–2660. https://doi.org/10.2174/156802611798040732
17. Konovalov B, Živković MD, Milovanović JZ, et al (2018) Synthesis, cytotoxic activity and DNA interaction studies of new dinuclear platinum(ii) complexes with an aromatic 1,5-naphthyridine bridging ligand: DNA binding mode of polynuclear platinum(ii) complexes in relation to the complex structure. Dalt Trans 47:15091–15102. https://doi.org/10.1039/C8DT01946K
18. Neidle S (2009) The structures of quadruplex nucleic acids and their drug complexes. Curr Opin Struct Biol 19:239–250. https://doi.org/10.1016/j.sbi.2009.04.001

19. Marcon G, Messori L, Orioli P (2002) Gold(III) complexes as a new family of cytotoxic and antitumor agents. Expert Rev Anticancer Ther 2:337–346. https://doi.org/10.1586/14737140.2.3.337
20. Crooke ST, Mirabelli CK (1983) Molecular mechanisms of action of auranofin and other gold complexes as related to their biologic activities. Am J Med 75:109–113. https://doi.org/10.1016/0002-9343(83)90482-5
21. Ronconi L, Marzano C, Zanello P, et al (2006) Gold(III) dithiocarbamate derivatives for the treatment of cancer: Solution chemistry, DNA binding, and hemolytic properties. J Med Chem 49:1648–1657. https://doi.org/10.1021/jm0509288
22. Radisavljević S, Scheurer A, Bockfeld D, et al (2021) New mononuclear gold(III) complexes: Synthesis, characterization, kinetic, mechanistic, DNA/BSA/HSA binding, DFT and molecular docking studies. Polyhedron 209:. https://doi.org/10.1016/j.poly.2021.115446
23. Radisavljević S, Kesić A, Ćoćić D, et al (2023) New gold(III) chlorophenyl terpyridine complex: Biomolecular interactions and anticancer activity against human oral squamous cell carcinoma. Appl Organomet Chem 37:1–19. https://doi.org/10.1002/aoc.6922
24. Dimiza F, Fountoulaki S, Papadopoulos AN, et al (2011) Non-steroidal antiinflammatory drug-copper(II) complexes: Structure and biological perspectives. Dalt Trans 40:8555–8568. https://doi.org/10.1039/c1dt10714c
25. Dimiza F, Perdih F, Tangoulis V, et al (2011) Interaction of copper(II) with the non-steroidal anti-inflammatory drugs naproxen and diclofenac: Synthesis, structure, DNA- and albumin-binding. J Inorg Biochem 105:476–489. https://doi.org/10.1016/j.jinorgbio.2010.08.013
26. Cócić D, Jovanović-Stević S, Jelić R, et al (2020) Homo- And hetero-dinuclear Pt(ii)/Pd(ii) complexes: Studies of hydrolysis, nucleophilic substitution reactions, DNA/BSA interactions, DFT calculations, molecular docking and cytotoxic activity. Dalt Trans 49:14411–14431. https://doi.org/10.1039/d0dt02906h
27. Becke AD (1993) Density-functional thermochemistry. III. The role of exact exchange. J Chem Phys 98:5648–5652. https://doi.org/10.1063/1.464913
28. Andrae D, Häußermann U, Dolg M, et al (1990) Energy-adjusted ab initio pseudopotentials for the second and third row transition elements. Theor Chim Acta 77:123–141. https://doi.org/10.1007/BF01114537
29. Weigend F, Ahlrichs R (2005) Balanced basis sets of split valence, triple zeta valence and quadruple zeta valence quality for H to Rn: Design and assessment of accuracy. Phys Chem Chem Phys 7:3297–3305. https://doi.org/10.1039/b508541a
30. M. J. Frisch, G. W. Trucks, H. B. Schlegel, G. E. Scuseria, M. A. Robb, J. R. Cheeseman, G. Scalmani, V. Barone, B. Mennucci, G. A. Petersson, H. Nakatsuji, M. Caricato, X. Li, H. P. Hratchian, A. F. Izmaylov, J. Bloino, G. Zheng, J. L. Sonnenberg, M. Had and DJF (2010) Gaussian 09
31. Thomsen R, Christensen MH (2006) MolDock: A new technique for high-accuracy molecular docking. J Med Chem 49:3315–3321. https://doi.org/10.1021/jm051197e

32. Milutinović M, Stanković M, Cvetković D, et al (2015) The Molecular Mechanisms of Apoptosis Induced by Allium flavum L. and Synergistic Effects with New-Synthesized Pd(II) Complex on Colon Cancer Cells. J Food Biochem 39:238–250. https://doi.org/10.1111/jfbc.12123
33. Ćurčić MG, Stanković MS, Mrkalić EM, et al (2012) Antiproliferative and proapoptotic activities of methanolic extracts from ligustrum vulgare L. as an individual treatment and in combination with palladium complex. Int J Mol Sci 13:2521–2534. https://doi.org/10.3390/ijms13022521
34. Baskić D, Popović S, Ristić P, Arsenijević NN (2006) Analysis of cycloheximide-induced apoptosis in human leukocytes: Fluorescence microscopy using annexin V/propidium iodide versus acridin orange/ethidium bromide. Cell Biol Int 30:924–932. https://doi.org/10.1016/j.cellbi.2006.06.016
35. Nikodijević DD, Jovankić J V., Cvetković DM, et al (2021) L-amino acid oxidase from snake venom: Biotransformation and induction of apoptosis in human colon cancer cells. Eur J Pharmacol 910:. https://doi.org/10.1016/j.ejphar.2021.174466
36. Podunavac-Kuzmanovic S, Vojinovic L (2003) Synthesis and physico-chemical characterization of zinc(II), nickel(II) and cobalt(II) complexes with 2-phenyl-2-imidazoline. Acta Period Technol 148:119–124. https://doi.org/10.2298/apt0334119p
37. Despaigne AAR, Da Silva JG, Da Costa PR, et al (2014) ROS-mediated cytotoxic effect of copper(II) hydrazone complexes against human glioma cells. Molecules 19:17202–17220. https://doi.org/10.3390/molecules191117202
38. Mihajlović K, Joksimović N, Radisavljević S, et al (2022) Examination of antitumor potential of some acylpyruvates, interaction with DNA and binding properties with transport protein. J Mol Struct 1270:. https://doi.org/10.1016/j.molstruc.2022.133943
39. Tarushi A, Lafazanis K, Kljun J, et al (2013) First- and second-generation quinolone antibacterial drugs interacting with zinc(II): Structure and biological perspectives. J Inorg Biochem 121:53–65. https://doi.org/10.1016/j.jinorgbio.2012.12.009
40. Metcalfe C, Rajput C, Thomas JA (2006) Studies on the interaction of extended terpyridyl and triazine metal complexes with DNA. J Inorg Biochem 100:1314–1319. https://doi.org/10.1016/j.jinorgbio.2006.03.005
41. Tarushi A, Polatoglou E, Kljun J, et al (2011) Interaction of Zn(ii) with quinolone drugs: Structure and biological evaluation. Dalt Trans 40:9461–9473. https://doi.org/10.1039/c1dt10870k
42. Nardon C, Boscutti G, Fregona D (2014) Beyond platinums: Gold complexes as anticancer agents. Anticancer Res 34:487–492
43. Porchia M, Pellei M, Marinelli M, et al (2018) New insights in Au-NHCs complexes as anticancer agents. Eur J Med Chem 146:709–746. https://doi.org/10.1016/j.ejmech.2018.01.065
44. Mirzadeh N, Reddy TS, Bhargava SK (2019) Advances in diphosphine ligand-containing gold complexes as anticancer agents. Coord Chem Rev 388:343–359. https://doi.org/10.1016/j.ccr.2019.02.027
45. Van Der Westhuizen D, Bezuidenhout DI, Munro OQ (2021) Cancer molecular biology and strategies for the design of cytotoxic gold(i) and gold(iii) complexes: A tutorial review. Dalt Trans 50:17413–

17437. https://doi.org/10.1039/d1dt02783b

46. Khan TM, Gul NS, Lu X, et al (2019) In vitro and in vivo anti-tumor activity of two gold(III) complexes with isoquinoline derivatives as ligands. Eur J Med Chem 163:333–343. https://doi.org/10.1016/j.ejmech.2018.11.047
47. Milutinović MG, Milivojević NN, Đorđević NM, et al (2022) Gold(III) Complexes with Phenanthroline-derivatives Ligands Induce Apoptosis in Human Colorectal and Breast Cancer Cell Lines. J Pharm Sci 111:3215–3223. https://doi.org/10.1016/j.xphs.2022.09.021
48. Augello G, Azzolina A, Rossi F, et al (2023) New Insights into the Behavior of NHC-Gold Complexes in Cancer Cells. Pharmaceutics 15:1–12. https://doi.org/10.3390/pharmaceutics15020466
49. Dasari TP S, Y Z (2015) Antibacterial Activity and Cytotoxicity of Gold (I) and (III) Ions and Gold Nanoparticles. Biochem Pharmacol Open Access 04: https://doi.org/10.4172/2167-0501.1000199
50. Alhoshani A, Sulaiman AAA, Sobeai HMA, et al (2021) Anticancer activity and apoptosis induction of gold(III) complexes containing 2,2'-bipyridine-3,3'-dicarboxylic acid and dithiocarbamates. Molecules 26:. https://doi.org/10.3390/molecules26133973
51. Zarić MM, Čanović PP, Pirković MS, et al (2021) New gold pincer-type complexes induce caspase-dependent apoptosis in human cancer cells in vitro. Vojnosanit Pregl 78:865–873. https://doi.org/10.2298/VSP190507002Z

Scheme

Scheme 1 is available in the Supplementary Files section.

Table

Table 7 is not available with this version.

Figures

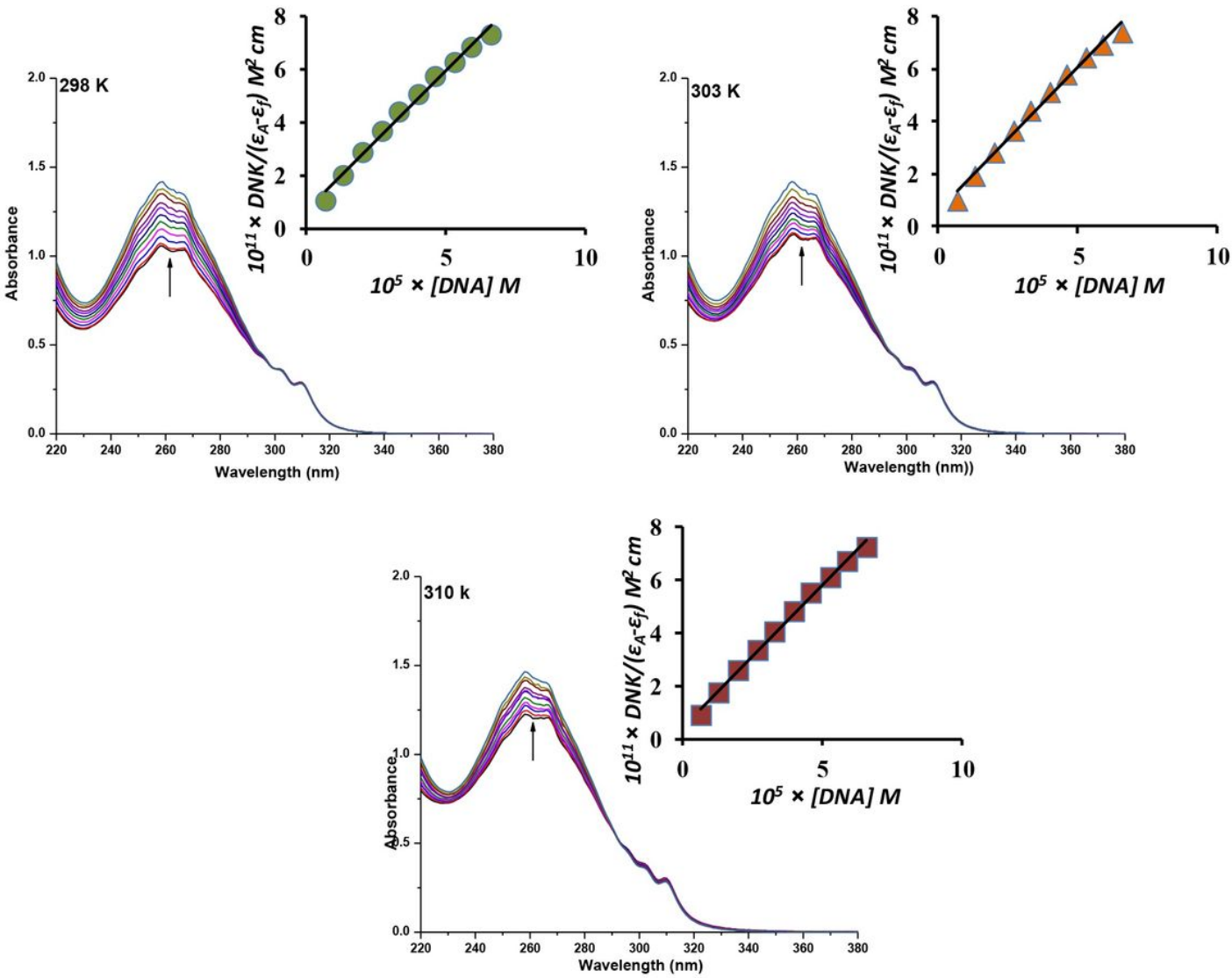

Figure 1

Absorption spectra of dinuclear gold(III) complex at different temperatures in PBS buffer upon addition of CT-DNA. [complex] = 1.35 × 10^{-5} M; [DNA] = 0.672 – 6.55 × 10^{-5} M. The change after addition of increasing concentration of DNA is presented with arrows. Insert: plot of [DNA]/(ε_a-ε_f) *vs.* [DNA]

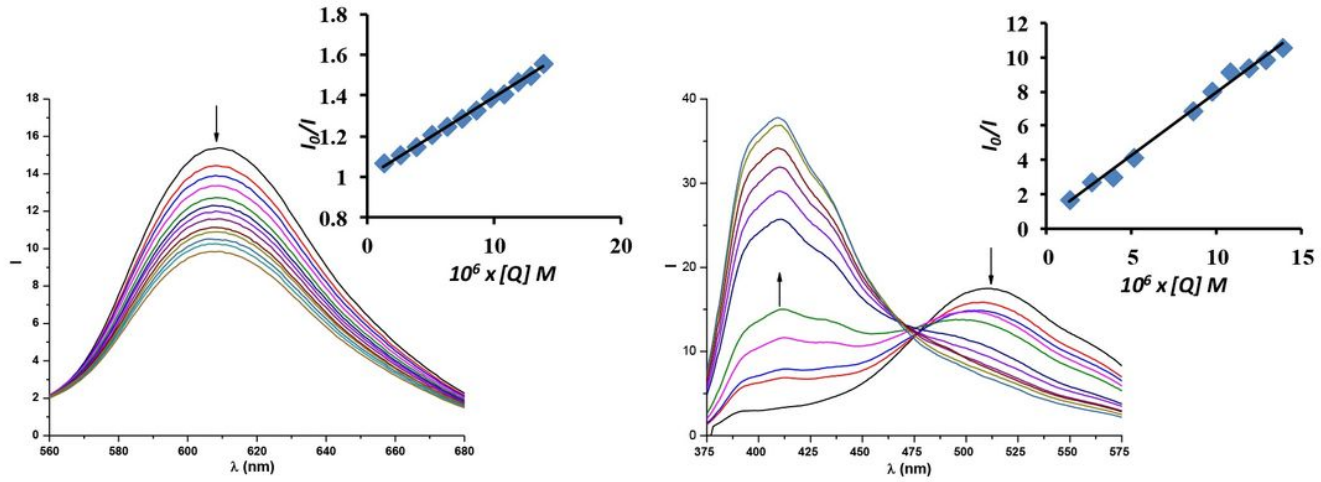

Figure 2

Emission spectra of EB-DNA (left)/HOE-DNA (right) in the presence of dinuclear gold(III) complex. [HOE/EB] = [DNA] = 6.73 μM; [complex] = (1.35 – 13.9 μM). Arrows show the change of the intensity upon increasing the concentration of dinuclear gold(III) complex. Insert graph: Plot of I_0/I *vs* Q

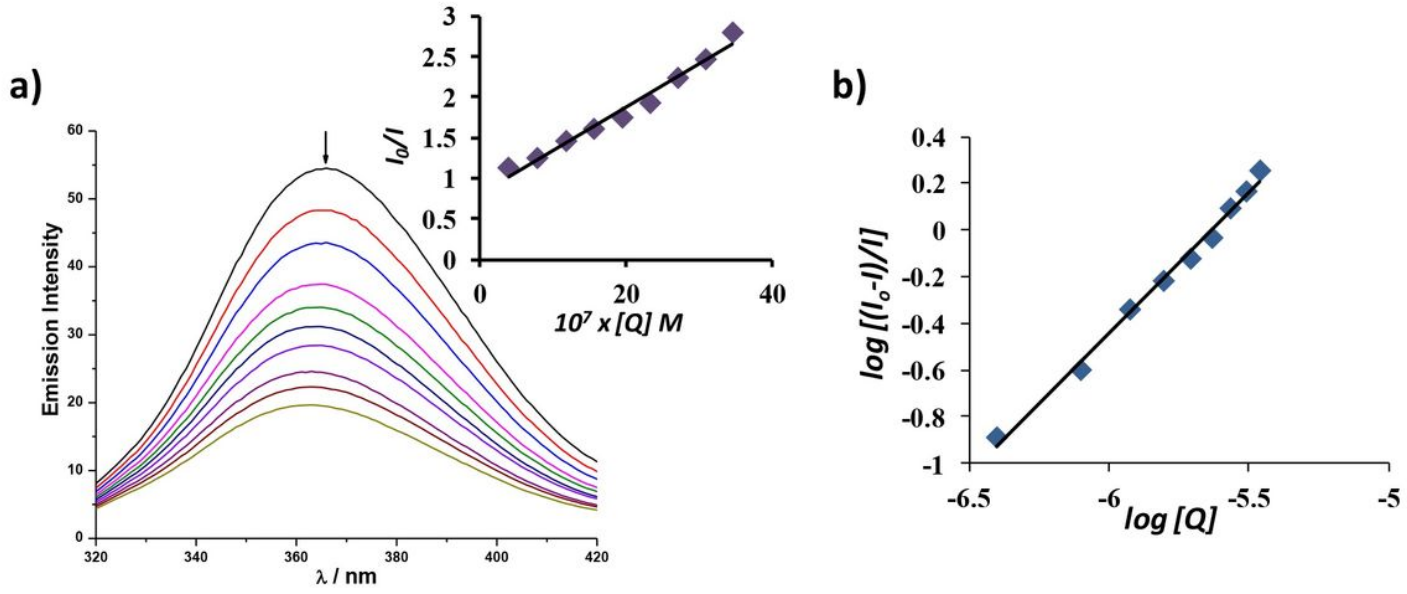

Figure 3

a) Emission spectra of BSA in the presence of dinuclear gold(III) complex. [BSA] = 2μM, [complex] = 0.398 – 3.47 μM; λ_{ex}= 295 nm. The arrow shows the intensity changes upon increasing the concentrations of complex. Insert: plots of I_0/I *vs.* [Q] **b)** Plot of $\log[I_0\text{-}I)/I]$ *vs.* log[Q] for gold(III) complex-BSA system at 298 K

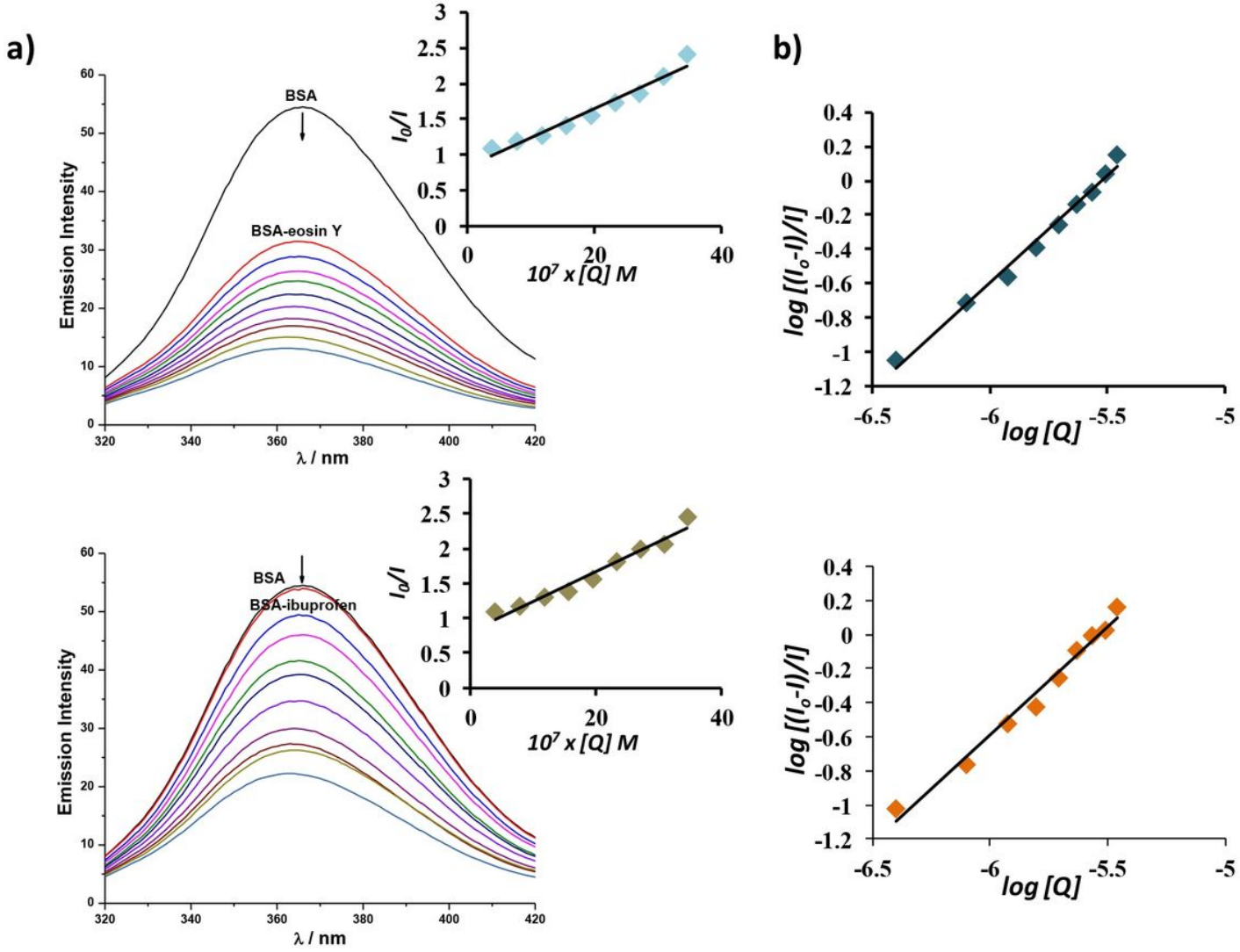

Figure 4

a) Emission spectra of BSA in the presence of site markers eosin Y (top) or ibuprofen (bottom) and dinuclear gold(III) complex. [BSA] = [eosin Y] = [ibuprofen] = 2μM, [complex] = 0.398 – 3.47 μM; λ_{ex}= 295 nm. The arrows show the intensity changes upon increasing the concentrations of complex. Insert: plots of I_0/I *vs.* [Q] **b)** Plot of log[I_0-I)/I] *vs.* log[Q] for BSA for eosin Y (top) and ibuprofen (bottom), at 298K

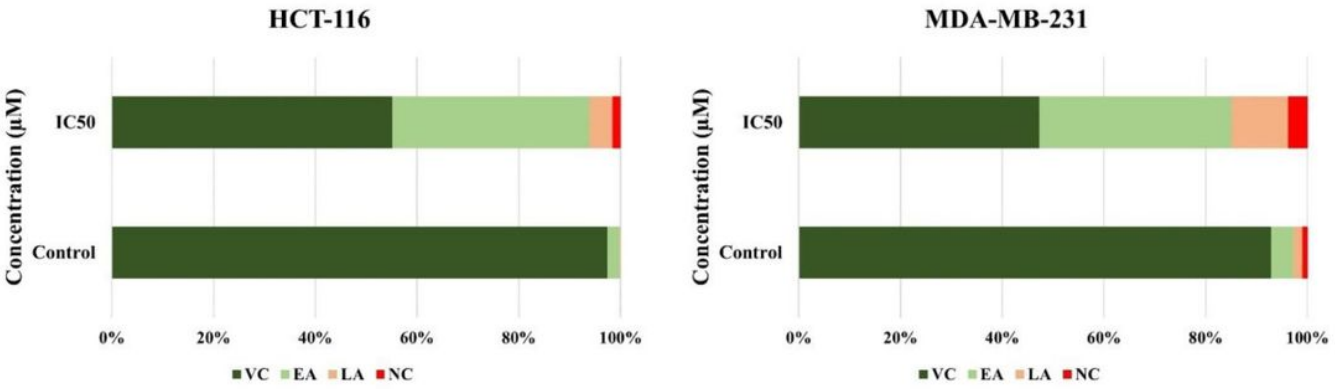

Figure 5

Percentages of viable cells (VC), cells in early (EA) and late (LA) stage of apoptosis, and necrosis (NC) in selected cancer cell lines – control values and cells treated by dinuclear gold(III) complex (IC_{50} value)

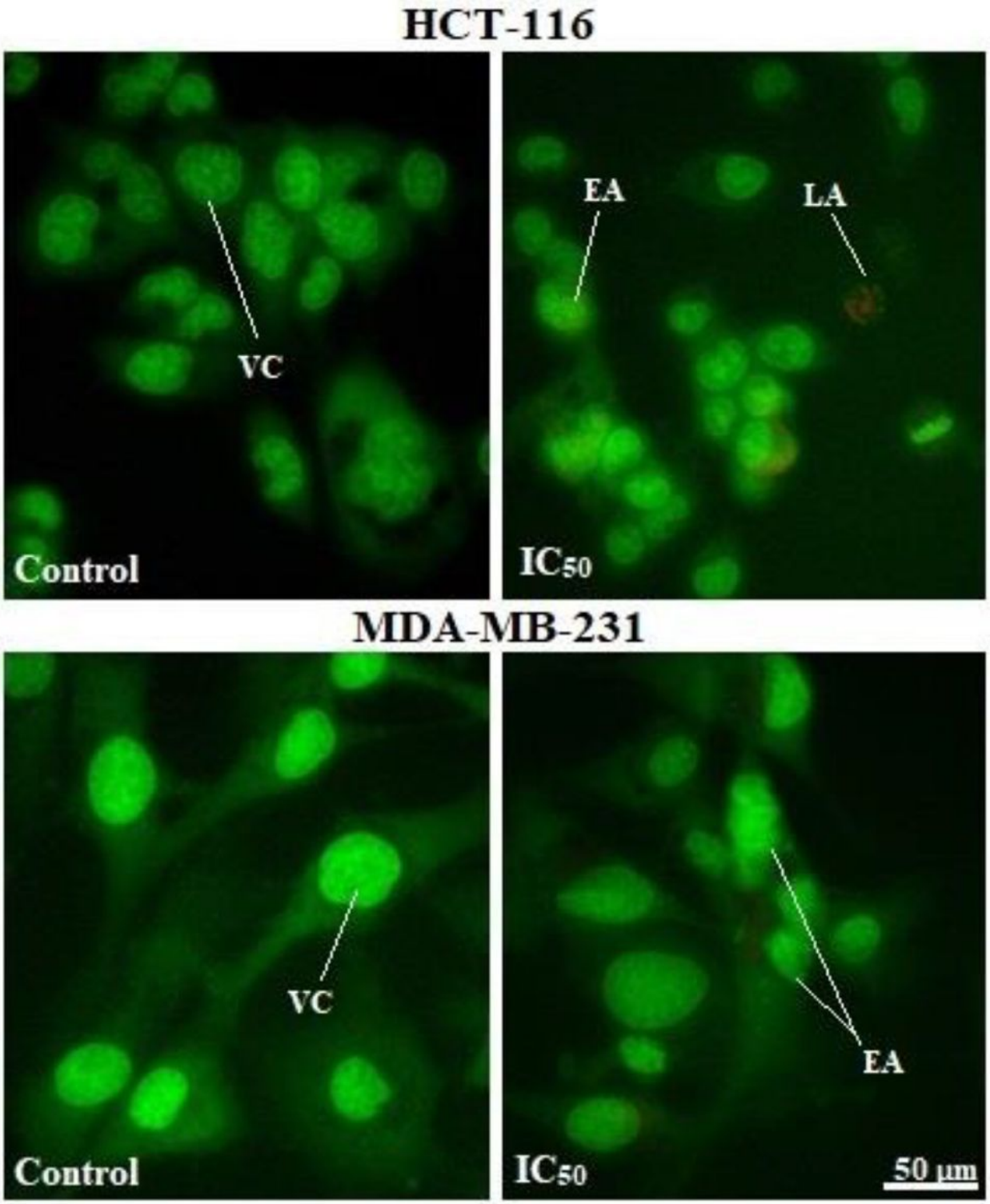

Figure 6

Micrographs from the fluorescent microscope (400x magnification). Cell morphology of control cells and cells treated by dinuclear gold(III) complex

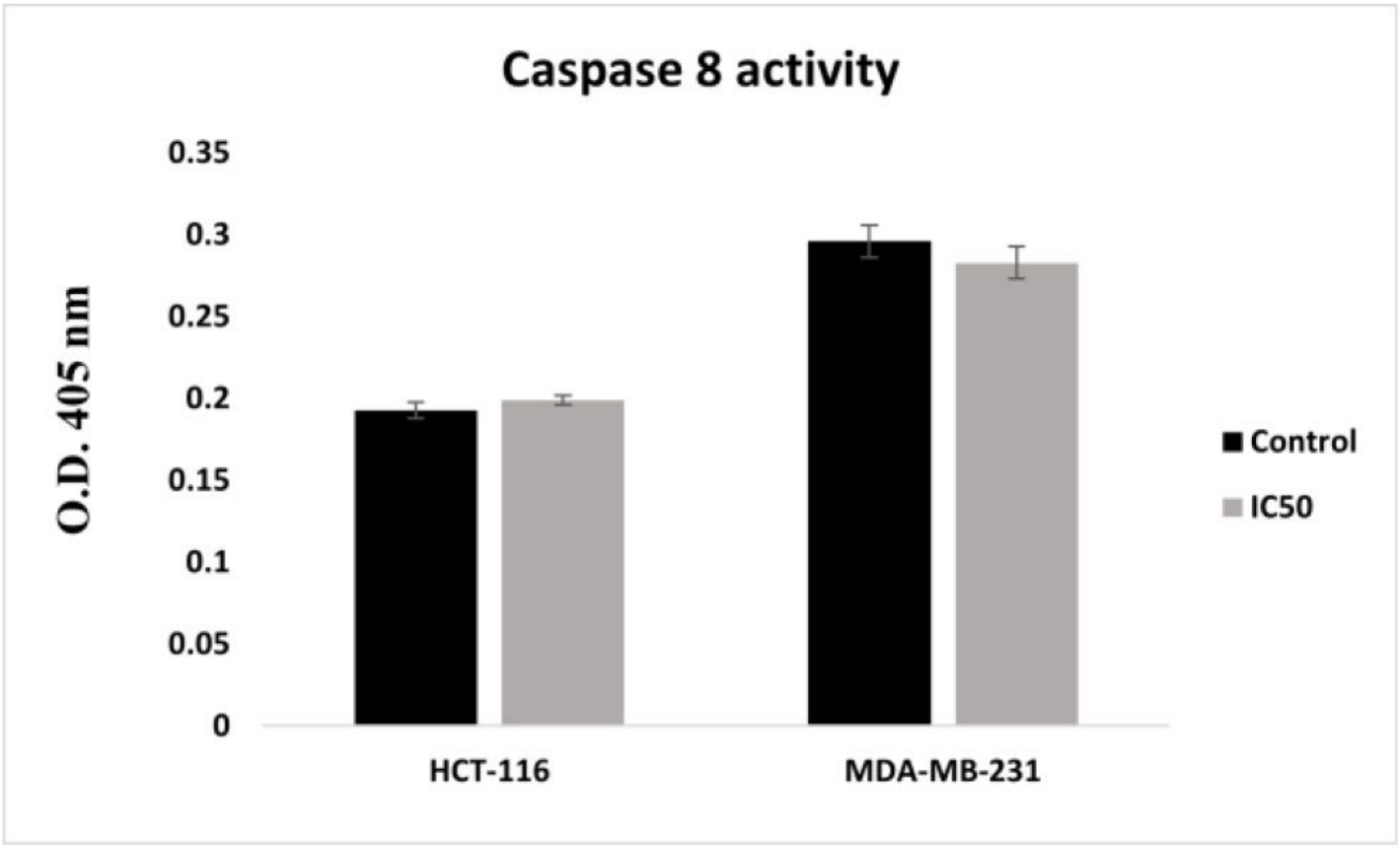

Figure 7

Caspase 8 activity in tested control and cells treated with dinuclear gold(III) complex (IC_{50} value), 24 h after treatment. +

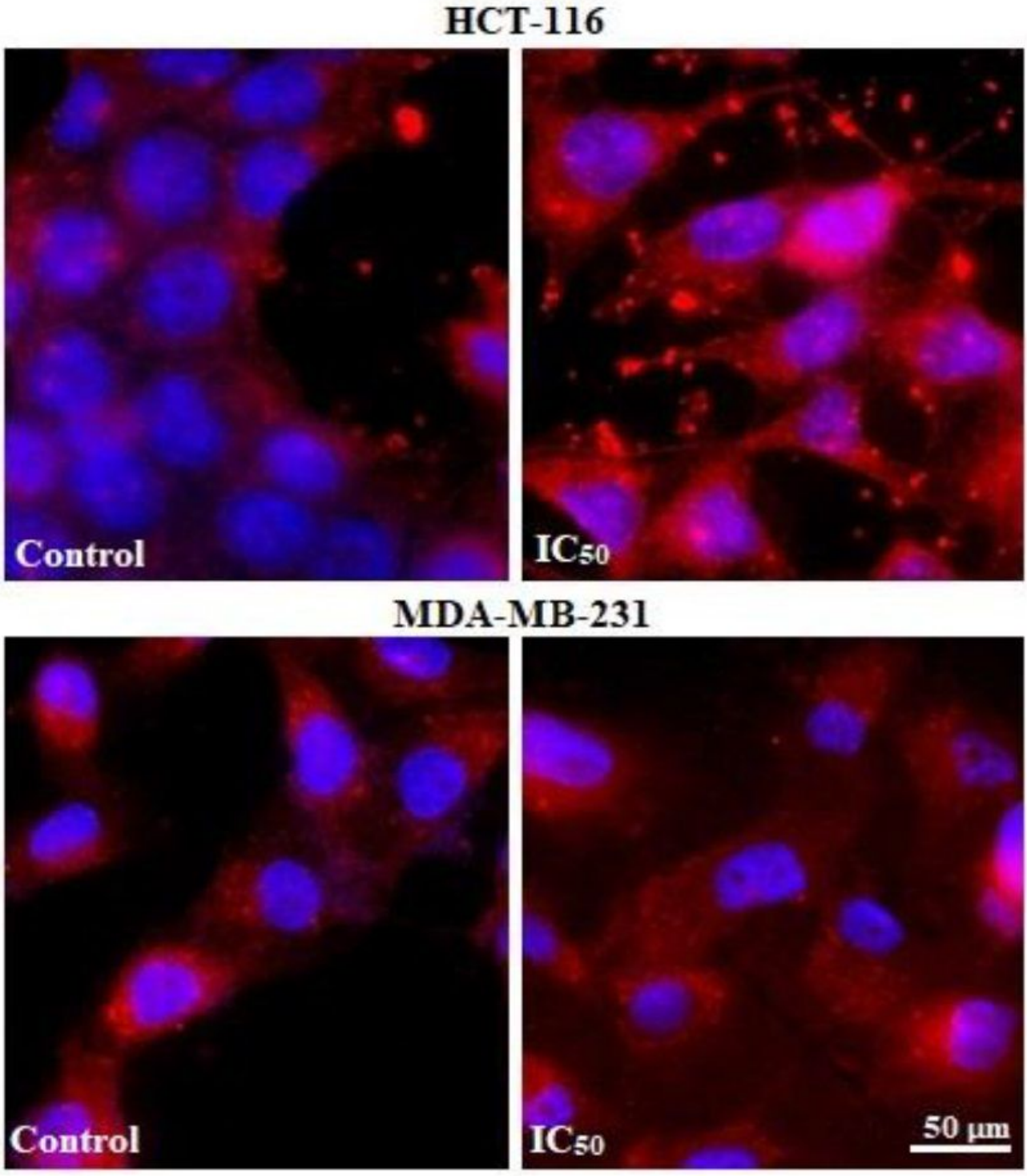

Figure 8

Micrographs (Fluorescence microscope, 600× magnification) with caspase 9 protein expression in tested control cells and cells treated with dinuclear gold(III) complex.

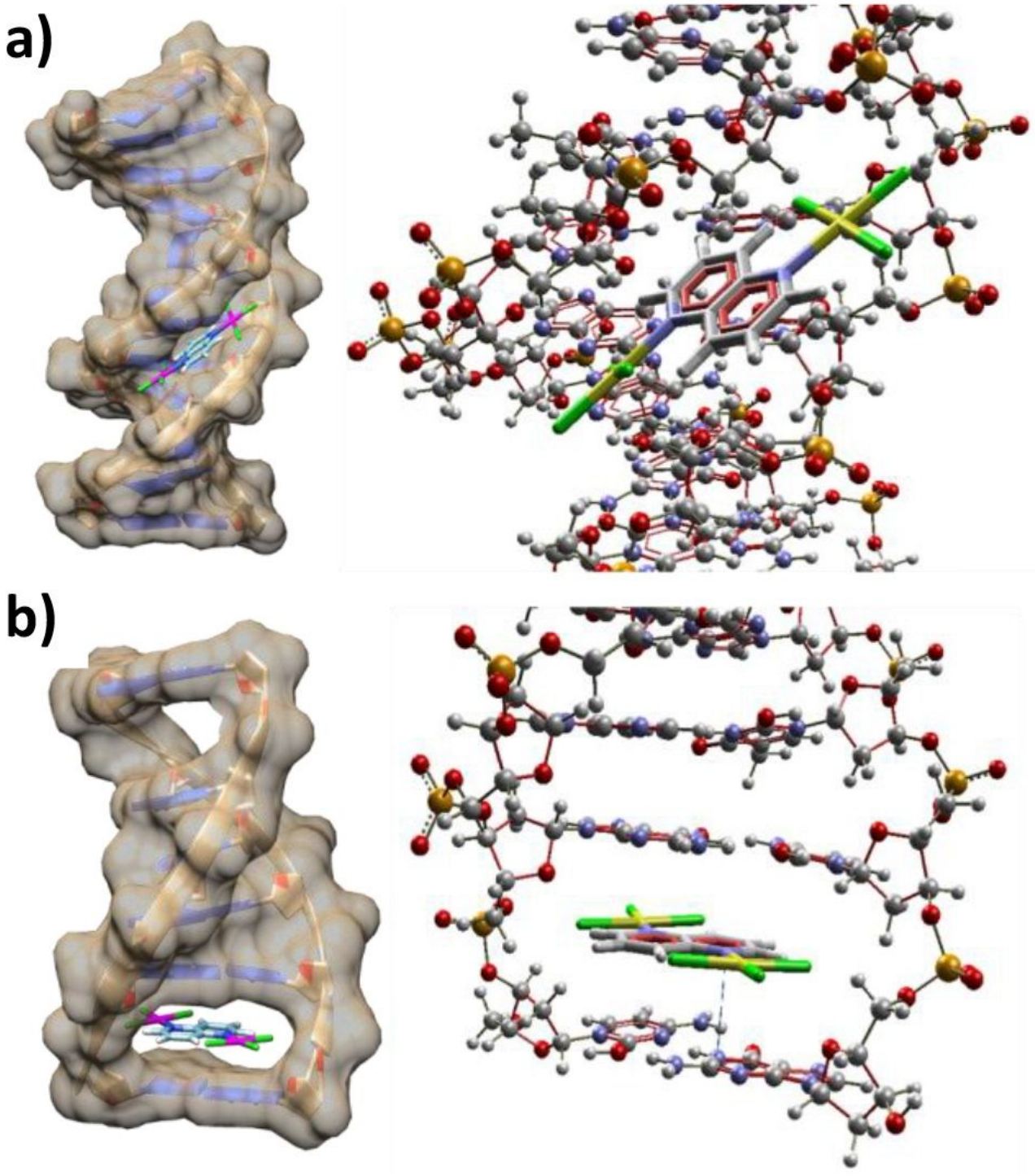

Figure 9

Computational docking model illustrating interactions between dinuclear gold(III) complex and DNA: A) with the canonical gap (1BNA); B) with the intercalation gap (1Z3F) (dotted lines display a possibility of forming hydrogen bonds)

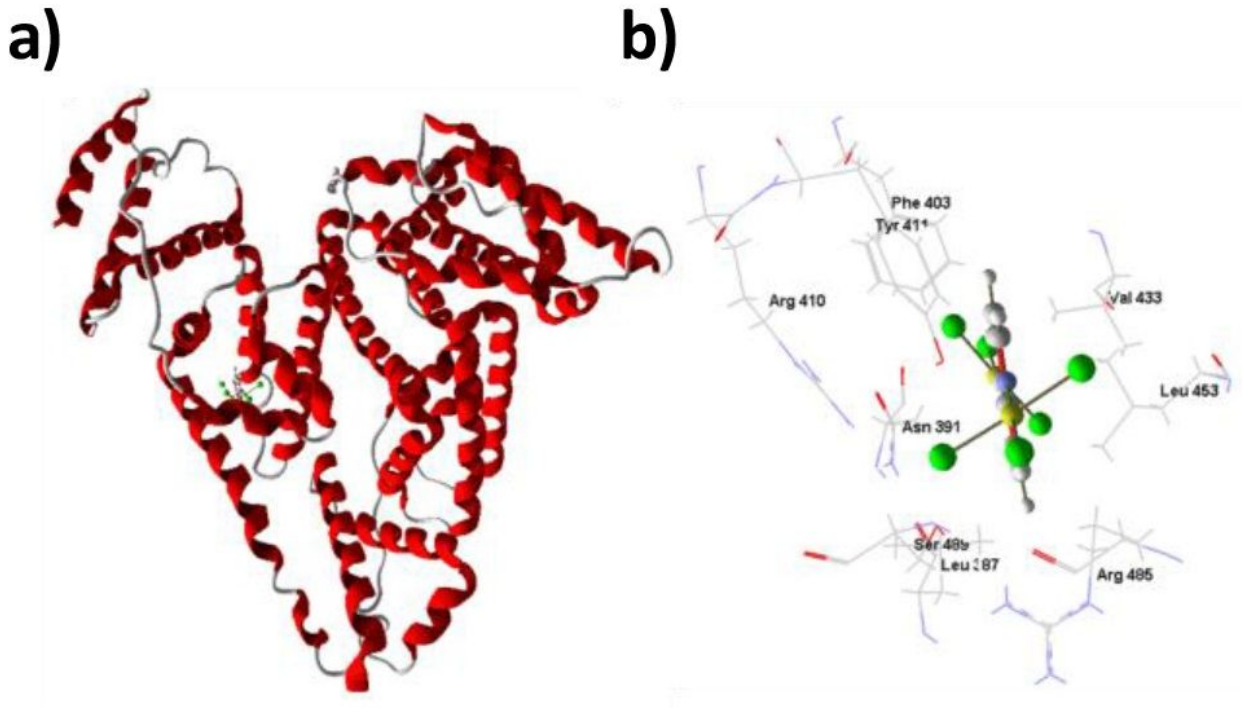

Figure 10

Best pose with BSA docked into a subdomain IIIA for dinuclear gold(III) complex according to Hbond values: A) molecular docking results illustrated regarding the BSA protein's backbone; B) binding site of investigated complexes on BSA protein and selected amino acid residues (selected by applying an energy threshold of 0.625) represented by stick models (hydrogen bonds are shown as blue dotted lines)

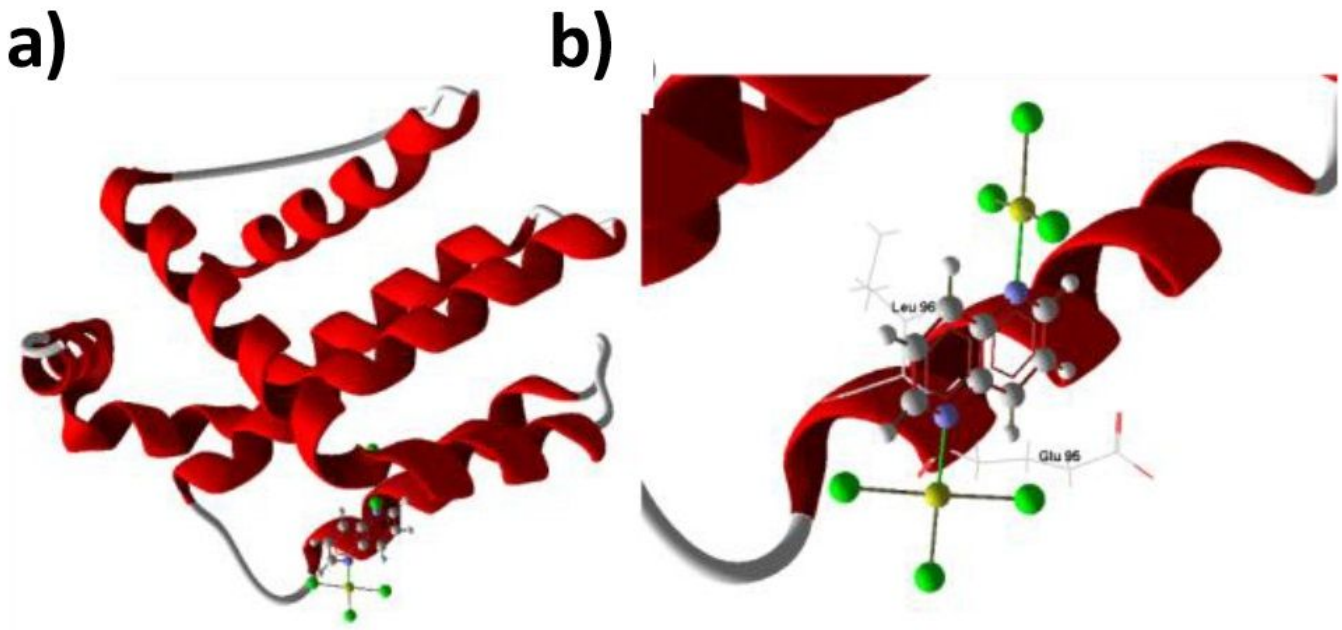

Figure 11

Best pose docked into protein Bcl-2 for dinuclear gold(III) complex according to Hbond values: A) molecular docking results illustrated regarding the Bcl-2 protein's backbone; B) binding site of investigated complex on Bcl-2 protein and selected amino acid residues (selected by applying an energy threshold of 0.625) represented by stick models (hydrogen bonds are shown as blue dotted lines)

Supplementary Files

This is a list of supplementary files associated with this preprint. Click to download.

- Scheme1.jpg
- Supportingdata.docx